Int. J. Cancer: **108,** 780–789 (2004)

Publication of the International Union Against Cancer

LOADING MITOMYCIN C INSIDE LONG CIRCULATING HYALURONAN TARGETED NANO-LIPOSOMES INCREASES ITS ANTITUMOR ACTIVITY IN THREE MICE TUMOR MODELS

Dan PEER and Rimona MARGALIT*

Department of Biochemistry, The George S. Wise Life Science Faculty, Tel-Aviv University, Tel-Aviv, Israel

The frequent overexpression of the hyaluronan receptors CD44 and RHAMM in cancer cells opens the door for targeting by the naturally-occurring high-M_r hyaluronan. This is the first time effective *in vivo* tumor targeting is reported for mitomycin C (MMC) loaded inside nano-sized hyaluronan-liposomes (denoted tHA-LIP). The severe adverse effects of free MMC made it a rational candidate for an effective targeted carrier. *In vitro*, loading MMC inside tHA-LIP increased drug potency 100-fold, in cells overexpressing, but not in cells underexpressing, hyaluronan receptors. Both types of liposomes were non-toxic and reduced MMC-related toxicity in healthy C57BL/6 mice. In 3 tumor models, BALB/c bearing C-26 solid tumors; C57BL/6 bearing B16F10.9 or (separately) D122 lung metastasis, tHA-LIP were long-circulating, 7-fold and 70-fold longer than nt-LIP and free MMC, respectively. tHA-LIP-mediated MMC accumulation in tumor-bearing lungs was 20% of injected dose, compared to 0.6% and 4% with free drug and nt-LIP, respectively. Tumor-free lungs showed low accumulation, irrespective of drug formulation. Key indicators of therapeutic responses, tumor progression, metastatic burden and survival, were superior ($p < 0.001$) in animals receiving MMC-loaded tHA-LIP, no treatment, MMC-loaded nt-LIP and free drug. In conclusion, tHA-LIP perform as tumor-targeted carriers, with promising prospects for treatment of tumors overexpressing hyaluronan receptors.

Key words: *mitomycin C, Hyaluronan, bioadhesive liposomes, targeting, drug delivery*

Hyaluronan (HA) is a naturally-occurring high M_r ($\sim 10^6$ Da) glycosaminoglycan composed of the repeating disaccharide β1,3*N*-acetyl glycosaminyl-β1,4 glucuronide. It exists in living systems in both free and complexed forms.[1–4] The hyaluronan-specific receptors CD44 and RHAMM are found at low levels on epithelial, hematopoietic and neuronal cells, and are overexpressed (one or both) in roughly all cancer types.[5–17]

CD44 appear to regulate lymphocyte adhesion to cells of high endothelial venules during lymphocyte migration,[6,10,14,17] a process that has many similarities to the metastatic dissemination of solid tumors[18] and is also implicated in regulating the proliferation of cancer cells.[19] A vital role has been suggested for CD44 in determining the fate of hematogenously disseminated melanoma cells.[19] Although hyaluronan receptors are expressed on a number of cell types in normal tissues, it seems that these cell types are either not in direct contact with the blood or require activation before they bind HA.[8,21] Perturbing the interaction of HA with its receptors was reported to reduce tumor formation, as was shown in animals bearing lung tumors established from CD44-expressing tumor cell lines.[20,22] Among agents found capable of such perturbation are an anti-CD44 mAb[23] and a CD44-receptor globulin.[23,24]

The relationships between tumor cells and hyaluronan receptors indicate that it may be possible to recruit hyaluronan for active targeting of carrier-loaded anticancer drugs, to tumors that are outside the RES. Positioned on the surface of a carrier, hyaluronan can endow the system with a critical trait for successful targeting: high affinity to recognition sites at the tumor. This provides for binding and retention of the drug-loaded carrier at the tumor, over a sufficient time span to deliver enough drug for efficacious therapy. Yet the forces driving carrier binding to recognition sites operate at short range and cannot, on their own, pull particles out of the circulation into the tumor. To reach the close proximity at which such binding can take place, the particles have to extravasate. To make the most of the extravasation, recognition and binding, to deliver efficacious drug doses to the tumor, requires the carriers to also be long-circulating.

The rather leaky vascular system reported for many tumors[25,26] allows particulate carriers, such as liposomes, some measure of extravasation from the circulation into the tumor. For liposomes it was shown that a small size, especially if combined with a hydrophilic coat such as PEG, provides long retention in circulation.[25–30] Yet the hydrophilic coat does not endow liposomes with high affinity to tumor-localized recognition sites. Efforts are underway to modify the liposomal surface with 2 agents, either bound individually or linked to one another, one responsible for long-term circulation and the other for high affinity to tumor sites.[31,32] Future prospects of this approach depend on whether the risks of mutual interferences can be satisfactorily resolved.

To endow liposomes with high affinity to recognition sites at designated therapeutic targets, we have previously developed "bioadhesive liposomes." These liposomes are surface-modified by covalent anchoring of bioadhesive macromolecules, selected from collagen, gelatin, EGF and hyaluronan, to their surface.[33–38] It was shown, *in vitro*, that the bioadhesive systems, especially the hyaluronan-liposomes, bind with high affinity to cells and to extracellular matrices carrying the appropriate recognition sites.[33–38] Designed originally for local (topical or regional) administration, we hypothesized that the particular species in which the bioadhesive ligand is the high-M_r naturally-occurring hyaluronan, may also be suitable for systemic administration, in particular for tumor chemotherapy. This was based on the rationale that surface-bound hyaluronan, although a single agent, may act in 2 roles: as the hydrophilic coat promoting long circulation, and as a targeting agent, docking the liposomes (through high affinity binding) at the membranes of tumor cells that overexpress hyaluronan receptors. Tumor regions are often also richer in ECM,[1] which may provide additional recognition sites for hyaluronan-liposomes. To test this hypothesis we set out to study the anti-tumor activity of mitomycin C (MMC), encapsulated in small unilamellar liposomes, with

Abbreviations: CH, cholesterol; DOC, deoxycholate; EDC, ethyl-dimethyl-aminopropyl-carbodiimide; HA, hyaluronan; MLV, multilamellar vesicles; MMC, mitomycin C; nt-LIP, non-targeted (regular liposomes); PBS, phosphate buffered saline; PC, phosphatidylcholine; PE, phosphatidylethanolamine; PEG, polyethyleneglycol; tHA-LIP, targeted hyaluronan-liposomes; ULV, unilamellar vesicles.

*Correspondence to: Department of Biochemistry, The George S. Wise Life Science Faculty, Tel-Aviv University, Tel-Aviv, 69978, Israel. Fax: +972-3-6406834. E-mail: rimona@post.tau.ac.il

Received 1 July 2003; Revised 14 August 2003; Accepted 26 August 2003

DOI 10.1002/ijc.11615

hyaluronan bound to their surface (denoted targeted hyaluronan-liposomes, abbreviated to tHA-LIP).

MMC is frequently first choice treatment for superficial-bladder and lung cancers, and a key component in combination chemotherapy for the treatment of breast, colorectal and prostate cancers.[39–42] In another therapeutic indication, it is applied as an antiproliferative agent to prevent abnormal healing of surgical wounds by slowing down excessive fibroblast proliferation, as in the case of glaucoma filtration surgery.[43] Despite its therapeutic advantages, treatment with MMC is severely hindered by undesirable side effects such as bone marrow suppression and gastrointestinal damage, which occur when the drug is administered (or allowed to gain access) into the circulation.[41,44] Efforts were made to formulate MMC and lipophilic MMC derivatives in soluble and in microparticulate carriers, such as liposomes and microspheres.[45–50] Unfortunately, these endeavors have met with limited therapeutic success *in vitro* and *in vivo*, and were often associated with decreased drug potency.[45–50] The major limitation to liposomal MMC being poor encapsulation (<5%),[47,48] we set out to try anew formulation of this drug in liposomes, employing our recently developed new procedure.[51,52]

We report here the results of our molecular, *in vitro* and *in vivo* studies of MMC-loaded tHA-LIP. In both *in vitro* and *in vivo* studies, performance of this test formulation, was compared to free MMC and to MMC encapsulated in non-targeted (*i.e.*, regular) liposomes (abbreviated to nt-LIP). The latter were similar in all respects to the targeted systems, except absence of the hyaluronan coating. The *in vitro* studies were conducted in cell lines that overexpress activated, and that express low or non-activated, HA receptors. The *in vivo* studies were conducted in several mouse tumor models, C-26 solid tumors, B16F10.9, and D122 lung metastasis and lung tumors, investigating pharmacokinetics, biodistribution, therapeutic responses and survival. We also evaluated subacute toxicity of drug-loaded and drug-free tHA-LIP in healthy mice, and compared those to equivalent systems of nt-LIP and free drug. This is the first time hyaluronan-liposomes were evaluated *in vivo* and shown to have high potential in cancer therapeutics.

MATERIAL AND METHODS

Chemicals

High-purity soybean phosphatidylcholine (PC) (Phospholipon 100) was a kind gift of Nattermann Phospholipid GMBH (Germany). All other high-purity lipids, ethyl-dimethyl-aminopropyl-carbodiimide (EDC), 3-(4,5-Dimethylthiazol-2-yl)-2,5-diphenyl-2H-tetrazolium bromide (MTT) and Trypan Blue, were purchased from Sigma (St. Louis, MO). Mitomycin C (MMC) was a kind gift from Dexon Ltd. (Israel). Hyaluronan (from bovine trachea) was a kind gift from Hyal Pharmaceutical Corporation (Canada). Fluorescein-labeled hyaluronan (from bovine trachea) was from Calbiochem (USA). Cell culture plates and dishes were from Corning (Corning, NY). Materials for cell cultures (specified below) were from Biological Industries (Beit Haemek, Israel). Dialysis tubing (molecular weight cutoff of 12,000–14,000) was from Spectrum Medical Industries (Los Angeles, CA). Polycarbonate membranes were from Nucleopore (Pleasanton, CA). All other reagents were of analytical grade.

Instruments

Centrifugation was carried out using a Beckman Optima TLX, Tabletop ultracentrifugation. Absorbance spectra were measured using a Cary UV-Visible spectrophotometer and a Thermomax microplate reader. Lyophilization was carried out with an Alpha 1-4 freeze drier (CHRIST, Germany). Liposome extrusion was carried out with the Lipex extrusion device (Vancouver, Canada). Liposomes were sized by dynamic light scattering using the ALV-NIBS High Performance Particle Sizer (Berlin, Germany). The net surface potential was determined with a Malvern Zetasizer IV (Malvern Instruments, Southborough, MA). HPLC was carried out with a Waters 717 auto sampler instrument with a PDA 996 detector. Confocal microscopy was done with a Zeiss LSM 510 instrument.

Preparation of drug-free and of MMC-loaded liposomes (nt-LIP and tHA-LIP)

nt-LIP. MLV were the raw material for the ULV used in our study. MLV composed of PC:PE:CH at mole ratios of 3:1:1, were prepared by the traditional lipid-film method.[33–38,51,52] Briefly, the lipids were dissolved in chloroform-methanol (3:1 vol/vol), evaporated to dryness under reduced pressure in a rotary evaporator and hydrated by the swelling solution that consisted of buffer alone (PBS) at the pH of 7.2. This was followed by extensive agitation using a vortex device and a 2-hr incubation in a shaker bath at 37°C. The MLV were extruded through the Lipex device, operated at room temperature and under nitrogen pressures of 200–500 psi. The extrusion was carried out in stages using progressively smaller pore-size membranes, with several cycles per pore-size, to achieve ULV in a final size range of <100 nm.

tHA-LIP. The surface modification was carried out on the nt-LIP, according to our procedures reported previously.[33–38,51,52] Briefly, HA was dissolved in water to a final concentration in the range of 2–5 mg/ml and preactivated by incubation with EDC, at pH 4 (controlled by titration with HCl) for 2 hr at 37°C. At the end of this step, the activated HA was added to a suspension of the drug-free nt-LIP, buffering by 0.1 M borate buffer to the final pH of 8.6. Incubation with the liposomes was continued for 24 hr at 37°C. At the end of the incubation, the liposomes were separated from excess reagents and by-products by centrifugation ($1.3 \times 10^5 g$, 4°C, 40 min) and repeated washings with PBS, reducing the pH back to physiological level. For the present studies the final product contained 57 μg HA/μmol lipid. A batch of nt-LIP underwent the same processes, except water at pH 4 were added instead of the activated HA. The tHA-LIP were lyophilized and kept at −18°C until further use**.** The lyophilization was carried out on 1.0 ml aliquots. Samples were frozen for 2–4 hr at −80°C and lyophilized for 48 hr.

Drug encapsulation

MMC-encapsulating nt-LIP were prepared as described above, except the swelling solution consisted of MMC dissolved in the PBS. MMC-encapsulating tHA-LIP were prepared by rehydration of the dried powder with an aqueous (pure water) solution of MMC.[51,52] The MMC concentrations in the swelling and in the rehydration solutions were in the range of 10 ng/ml–500 μg/ml. Rehydration was to the original pre-lyophilization liposome concentration, to retain original buffering and salinity status. Final liposome diameters were 75 ± 8 and 55 ± 6 nm, for the tHA-LIP and the nt-LIP, respectively.

Drug diffusion

Kinetics of drug efflux from the liposomal formulations were studied according to our procedures reported previously.[33–38,51,52] Briefly, a suspension of liposomes (0.5–1.0 ml) was placed in a dialysis sac and the sac was immersed in a constantly-stirred receiver vessel filled with drug-free buffer (PBS at pH 7.2), at vol 10- to 16-fold that of the sac. At designated periods, the dialysis sac was transferred from one receiver vessel to another, containing fresh (*i.e.*, drug-free) buffer. Drug concentration was assayed in each dialysate and in the sac (at the beginning and end of each experiment). To obtain a quantitative evaluation of drug release, experimental data were analyzed according to a previously-derived multi-pool kinetic model,[33–38,51,52] in which drug efflux from the sac into the reservoir occurs from a series of independent drug pools, one corresponding to free (*i.e.*, unencapsulated) drug, and all others to liposome-associated drug. The overall drug release corresponds to the following equation:

$$f(t) = \sum_{j=1}^{n} f_j (1 - \exp^{-k_j t}) \quad (1)$$

where f(t) is the cumulative drug that diffuses from the sac into the reservoir at time = t, normalized to the total drug in the system at time = 0, f_j is the fraction of the total drug in the system occupying the j'th pool at time = 0, and k_j is the rate constant for drug diffusion from the j'th pool.

Encapsulation efficiency

Defined as the ratio of entrapped drug to the total drug in the system, encapsulation efficiency can be determined by 2 independent methods. Method 1 is by centrifugation. Samples of complete liposome preparation (*i.e.*, containing both encapsulated and unencapsulated drug) are centrifuged as described above. The supernatant, containing the unencapsulated drug, is removed and the pellet, containing the encapsulated drug, is resuspended in drug-free buffer. Drug is assayed in the supernatant and in the pellet, as well as in the complete preparation. The results of these assays serve to calculate encapsulation efficiency as well as to verify conservation of matter. Method 2 uses data analysis of efflux kinetics. As discussed above, magnitudes of the parameter f_j are obtained through data analysis. When the efflux experiment is carried out on samples from the complete liposome preparation, the sum of f_j(s) for the pool(s) of encapsulated drug is also the efficiency of encapsulation.

Cell culture growth and maintenance

Monolayers of C-26, B16F10.9, D122, PANC-1, U2OS and CV-1 cells were grown in 100 × 20 mm dishes (Corning) as described previously.[34–37] The B16F10.9, PANC-1, and U2OS cells were cultured in DMEM. The CV-1 cells were maintained in DMEM H-21 (high glucose, 4.5 g/l) medium containing 10% FBS, 0.01 DMEM non-essential amino acids, 1% HEPES buffer (1 M) and 0.01 penicillin-streptomycin, 0.1 μm sterile filtered. C-26 and D122 cells were cultured in RPMI 1640. All cultures were maintained at 37°C in 5% CO_2 supplemented with 10% FCS, penicillin (10,000 U/ml), streptomycin (10 mg/ml) and L-glutamine (200 mM). Cells were transferred twice a week and were free of *Mycoplasma* contamination as determined by a *Mycoplasma* ELISA test (Boehringer Mannheim GmbH, Mannheim, Germany) carried out every 3 months. For all of the experiments, cells were harvested from subconfluent cultures using trypsin and were resuspended in fresh complete medium before plating. Viability of cultures used in the experiments were >90%, as determined by the Trypan blue method.

Liposome binding to cell monolayers

The experiments were carried out as described previously.[34–37] Briefly, cells were seeded onto 24-multiwell culture plates at densities in the range of 5×10^4–5×10^5 cells/ml and the experiments were carried out when the monolayers reached confluency. The cells, after washing with serum-free media, were incubated with the reaction mixture (triplicates for each data point), tHA-LIP or nt-LIP suspended in serum-free medium, for 60 min at room temperature. Upon termination, the reaction mixture in each well was diluted and aspirated, and the wells subjected to repeated extensive washings. After the last wash, the cells from each well were detached by trypsinization or lysed with 1 N NaOH. The well content was collected and assayed for cell-associated liposomes. Several wells in each plate served as controls, receiving binding buffer alone. The number of cells/well was quantitated for each experiment. The results were analyzed according to a Langmuir equation.[33–38]

Confocal microscopy

Cells were grown on cover slides. The formulations studied consisted of free fluorescein and fluorescein entrapped in each of the 2 liposome types, and of drug-free tHA-LIP containing fluorescein-labeled HA. Unencapsulated fluorescein was removed from the liposomal samples, and the fluorescein concentration was set equal, 15 μM, in all 3 formulations. Each formulation was incubated with the cells at room temperature for 1 hr. At the end of the incubation the cells were subjected to 6 washes with PBS and were fixed with mounting medium (Mounting medium with anti-fading agents, Biomeda Corp., CA). Excitation was at 488 nm and emission was measured using a band pass filter of 505–550 nm.

In vitro *cytotoxicity*

Twenty-four hours before an experiment, cells of the desired line were seeded onto 96-well multiwell culture plates at densities in the range of 1×10^4 cells/ml. The experiments were initiated on sub-confluent monolayers. The treatment media was selected from the following MMC formulations: (*i*) the test system, MMC-loaded tHA-LIP, (*ii*) MMC-loaded nt-LIP, (*iii*) free MMC, (*iv*) free MMC dissolved in a suspension of empty tHA-LIP and (*v*) free MMC dissolved in a suspension of empty nt-LIP. In addition, there were 3 drug-free controls, consisting of: (*vi*) no addition (*i.e.*, only the serum-supplemented growth medium), (*vii*) empty tHA-LIP and (*viii*) empty nt-LIP. In all formulations, the solvent was serum-supplemented cell growth medium.

The cells were incubated (under the usual growth conditions) with the selected treatment media for 4 hr, at the end of which the media was removed and the cells washed and fed with drug-free serum-supplemented growth media. The experiment was terminated 20 hr later and the quantity of viable cells was determined for each well.

In vivo *studies*

Animals were obtained from the animal breeding center, Tel Aviv University, Tel Aviv, Israel. Animals were maintained and treated according to NIH guidelines. All animal protocols were approved by the Tel-Aviv Institutional Animal Care and Use Committee.

*Subacute toxicity evaluation.*Tumor-free C57BL/6 male mice (5/group) were given a bolus injection of saline or of selected MMC formulations at the dose of 10 mg/kg body to the tail vein, on Days 0, 7, 14, 21 and 28 of the experiment, and the animals were weighed on a regular basis. The MMC formulations were those listed above under (*i*) to (*iii*) and (*vii*) to (*viii*). For histological changes, the mice were sacrificed on Day 30, 2 days after the last injection. The organs were fixed in 10% formalin and processed for light microscopy examination with H&E-phosphomolybdic acid light green stain. The following organs were examined: liver, spleen, kidney and stomach.

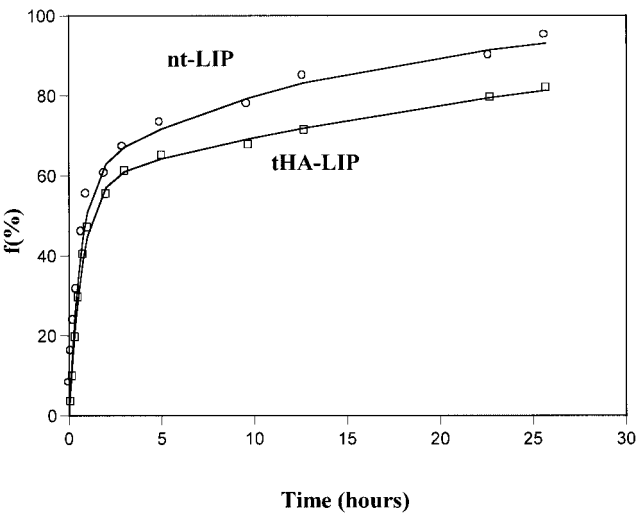

Figure 1 – Kinetics of MMC efflux from non-targeted liposomes (nt-LIP), and from hyaluronan targeted- liposomes (tHA-LIP). The points are experimental, each an average of duplicates, with SD (not shown) smaller than the symbol size. The solid curves are the theoretical expectations, the results of data processing according to equation (1) in the text (see Material and Methods) for the case of $n = 2$.

Tumor models

Solid tumor model. The protocol was adapted from[53] with minor changes. C-26 cells were implanted into the footpad of 8 weeks old female BALB/c mice (5×10^5 cells/mouse in 30 μl of Hank's buffer).

Lung metastasis models. The models and protocols were adapted from[54,55] with some minor changes. The selected cells, the B16F10.9 or D122, were administered i.v. into the tail vein of 12-week-old male C57BL/6 mice (5×10^5 cells /mouse in 50 μl PBS). Treatments (detailed below) were initiated on Day 1 post-tumor inoculation to maintain conditions of metastatic disease.

Lung tumor model. Same as the lung metastatic model with the B16F10.9 line, but treatment was initiated on Day 10, to allow for development of tumors.

Pharmacokinetics

Plasma clearance studies were carried out with the C-26 and the B16F10.9 tumor models (10 mice/group). The administered for-

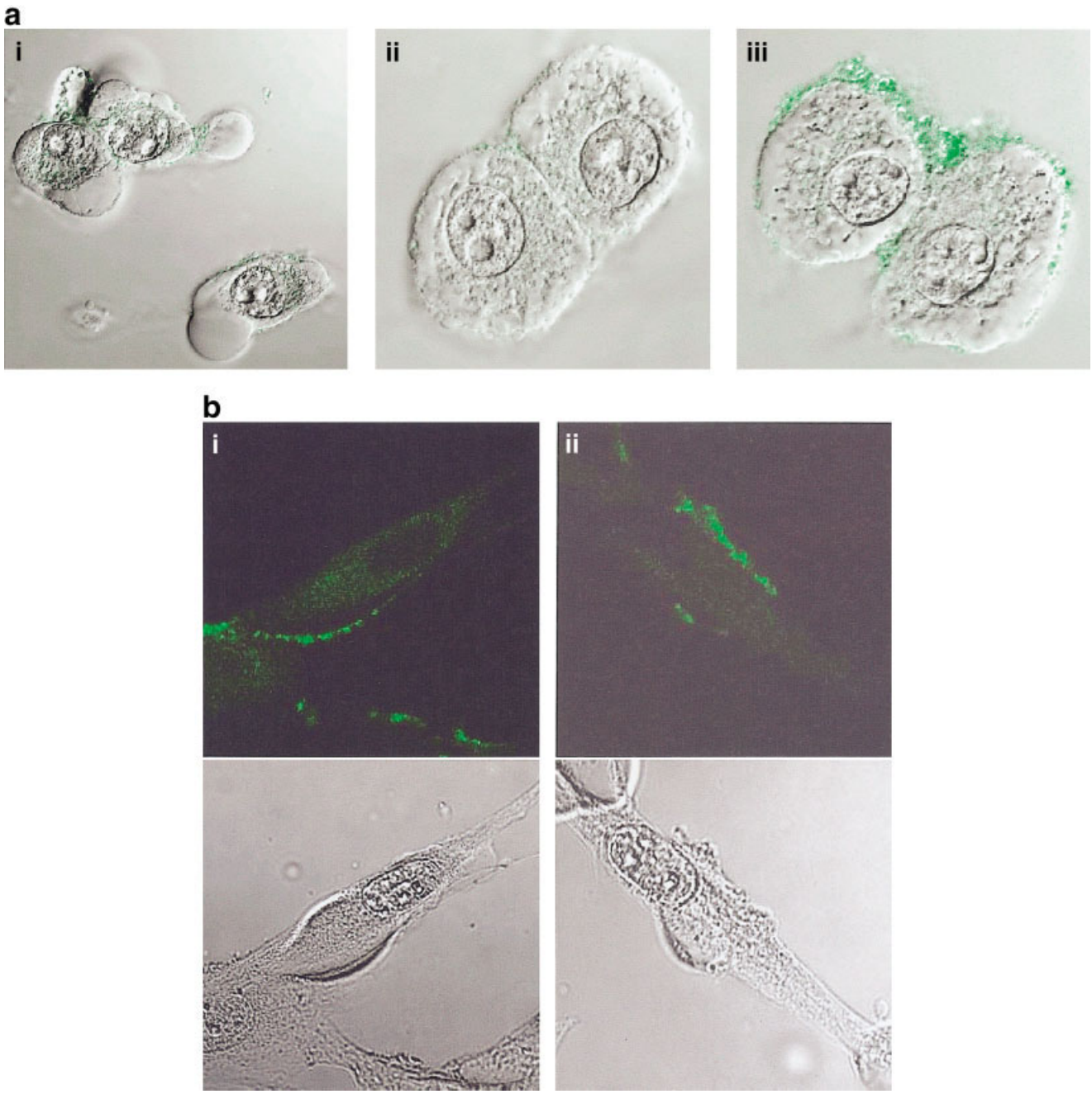

FIGURE 2 – confocal microscopy of B16F10.9 cells, incubated for one hour at room temperature with the following selected formulations (see Material and Methods for further details). (*a*) Cells incubated the following fluorescein formulations: (*i*) free fluorescein, (*ii*) fluorescein encapsulated in nt-LIP, (*iii*) fluorescein encapsulated in tHA-LIP. Unencapsulated fluorescein was removed from each of the liposomal formulations before incubation with the cells, and all formulations were equal in fluorescein concentration, 15 μM. Incubation was. (*b*) Fluorescence (*top panel*) and Namarsky (*bottom panel*) views of cells incubated with tHA-LIP. (*i*) Drug-free tHA-LIP containing fluorescein-labeled HA, (*ii*) fluorescein encapsulated in non-labeled tHA-LIP, as in (*a*,*iii*) above.

mulations were the test system MMC-loaded tHA-LIP, MMC-loaded nt-LIP and free MMC. Administration was by i.v. injection of 100 μl of the selected formulation to the lateral tail vein, using 26-gauge needles. All formulations were equal in the injected drug dose (10 mg/kg body). Blood samples were collected over a time span of 70 hr post-injection via retrobulbar puncture. The blood samples were immediately mixed with 250 μl of 0.5 mM EDTA-PBS, followed by a 5-min centrifugation at 200*g*. MMC was assayed in both cell and supernatant fractions. The pelleted cells and the supernatant from the first centrifugation were separated, and the cells were subjected to a wash (including re-centrifugation) in the EDTA-PBS solution. The supernatants from both runs were combined and assayed for MMC. Mitomycin C was extracted from the cells by incubation with 2.5 ml acidic isopropanol (81 mM HCl in isopropanol) for 4 hr at 4°C, followed by centrifugation under the same conditions specified above. The supernatants, containing the extracted MMC, were also subjected to assay and found to contain negligible amounts of MMC (<0.001% of injected dose). Calculation of area under the concentration versus time curve (AUC) values was carried out using the WinNonlin program (version 1.1; Pharsight Corporation, Mountain View, CA) by means of the noncompartmental analysis method.

Drug biodistribution

The experiment included 2 groups of C57BL/6 mice (15/group). One group was inoculated with B16F10.9 cells to bear lung tumors, the other group was of healthy mice. Each group was divided into 3 sub-groups (5/group), receiving a single i.v. dose of the following formulations on Day 10 from tumor inoculation: free MMC, MMC-loaded nt-LIP, and MMC-loaded tHA-LIP. Drug dose in all cases was 10 mg/kg body and details of administration are as listed above for the pharmacokinetics. Six hours post-injection the mice were anesthetized and sacrificed. Liver, spleen, kidneys and lungs were removed and each organ was examined by a pathologist blinded to the experimental groups involved. Each organ was then homogenized, MMC was extracted from it as described above for pharmacokinetics and assayed.

Lung metastasis Model I

C57BL/6 mice, inoculated with B16F10.9 cells, were divided into 4 groups (5/group), according to the following treatment formulations: saline, free MMC, MMC-loaded nt-LIP and MMC-loaded tHA-LIP. All drug-containing formulations were equal in dose, 10 mg/Kg body, and administration details were as described above under pharmacokinetics. Treatments were on Days 1, 5 and 9 from tumor inoculation. An additional group of untreated tumor-free mice served as control for normal lung weight and absence of lung metastasis. Twenty-one days post-tumor injection, all surviving animals were sacrificed. The lungs of all animals in the experiment (whether diseased or sacrificed) were removed, weighted and fixed in Bouin's solution. Lung weight increase was calculated by using the formula:[54] lung weight increase (%) = (tumor lung weight − normal lung weight)/normal lung weight × 100. Surface metastases were counted, using a dissecting microscope by a technician blinded to the experimental groups involved. Survival experiments were done according to the same protocol in a separate experiment.

Lung metastasis Model II

Studies with this model were similar in all to Model I above, except the animals were inoculated with D122 cells, and monitoring of therapeutic effects was through following animal survival.

Primary tumor growth

Animal groups (5/group), treatment formulations, drug doses and method of administration were as described above for the lung metastatic Model I. Treatments were initiated after the development of an easily palpable tumor (5 days), and given on Days 5, 12, 19 and 26 days post tumor inoculation. Tumor size was measured, using an electronic caliper, every other day for the next 30 days. Tumor volume was calculated by using the following formula:[53] tumor volume = $1/2(\text{width})^2 \times \text{length}$. Animal survival was monitored continuously, and the experiment was terminated on Day 115.

Quantitative determinations

For the molecular and *in vitro* experiments MMC was assayed by its absorption at 365 nm, in a 96-well plate, using a plate reader. For the pharmacokinetic studies MMC was assayed by HPLC with a PDA detector (365 nm).[51] Absorption coefficients for the drug in buffer and in 5% DOC were 0.0127 ml/μg and 0.0153 ml/μg, respectively. MMC absorption was linear in the range of 0–100 μg/ml. Assay samples in which the MMC concentrations were below detection limit were concentrated by lyophilization and redissolution in a final volume smaller than the original. The liposomes were quantitated by including a trace of ^{3}H-CH in the formulation. The quantity of viable cells was determined by: (*i*) the MTT test, recording the absorbencies in a plate reader, at 2 wavelengths, 550 and 650 nm,[56] (*ii*) total cell protein by the Bradford assay and (*iii*) the Trypan Blue method.

Statistics

The results are reported as mean ± SD for each group. Statistical significance was evaluated from two-tailed Student's *t*-tests.

RESULTS

Formulation properties: physicochemical, structural and in vitro *characterization*

MMC efflux from the liposomal formulations (Fig. 1) was processed according to equation (1) and found to fit the case of 2 drug pools (*i.e.*, $n = 2$) with a rather fast dissipation of unencapsulated MMC and significantly slower efflux of the encapsulated drug. The rate constants determined for the efflux of encapsulated MMC from nt-LIP and from tHA-LIP, $19.8(\pm 0.3) \times 10^{-3}$ hours^{-1} and $13.3(\pm 0.5) \times 10^{-3}$ hours^{-1}, correspond to half-lives of 35 and of 50 hr, respectively. The MMC encapsulation efficiencies, in good agreement between the two independent determination methods, were 38(±4)% and 53(±3)%, for the nt-LIP and the tHA-LIP, respectively. These results indicate that it is possible to achieve appreciable MMC encapsulation through elevation, at the stage of drug encapsulation, of liposome concentration. The latter was identified long ago as a key element in controlling encapsulation efficiencies.[33–38,51,52]

Zeta potentials of 0.3 mV and −12.5 mV were determined for nt-LIP and tHA-LIP, respectively. These magnitudes and directions fit with the lipid composition of the non-targeted particles and with the surface modification by the negatively charged hyaluronan in the case of the targeted systems. Anchoring hyaluronan to the liposomal surface did not impair its ability to bind to its receptors. This was verified by previous and by current thermodynamic binding studies to monolayers of cells carrying HA receptors, that yielded K_d magnitudes within the range of 0.05–0.6 nM HA,[34–38] quite similar to those reported for free HA.[57,58]

Retention of receptor affinity by liposome-anchored HA is also illustrated by the confocal microscopy results with B16F10.9 cells,

TABLE I – IN VITRO CYTOTOXICITY OF MITOMYCIN C AS FUNCTION OF FORMULATION[1]

Cell line	Free MMC	MMC/nt-LIP[2]	MMC/tHA-LIP[3]
CV-1	105	180	200
U2OS	70	150	160
B16F10.9	210	300	1.1
C26	105	270	1.8
D122	210	300	1.4
PANC-1	180	300	1.4

[1]IC_{50} (μm) was determined for each cell line after exposure to a series of drug concentrations using the transient protocol. SD values were <5% of the IC_{50} value ($n = 5$).–[2]nt-LIP, regular, non-targeted liposomes.–[3]tHA-Liposomes, targeted hyaluronan-liposomes.

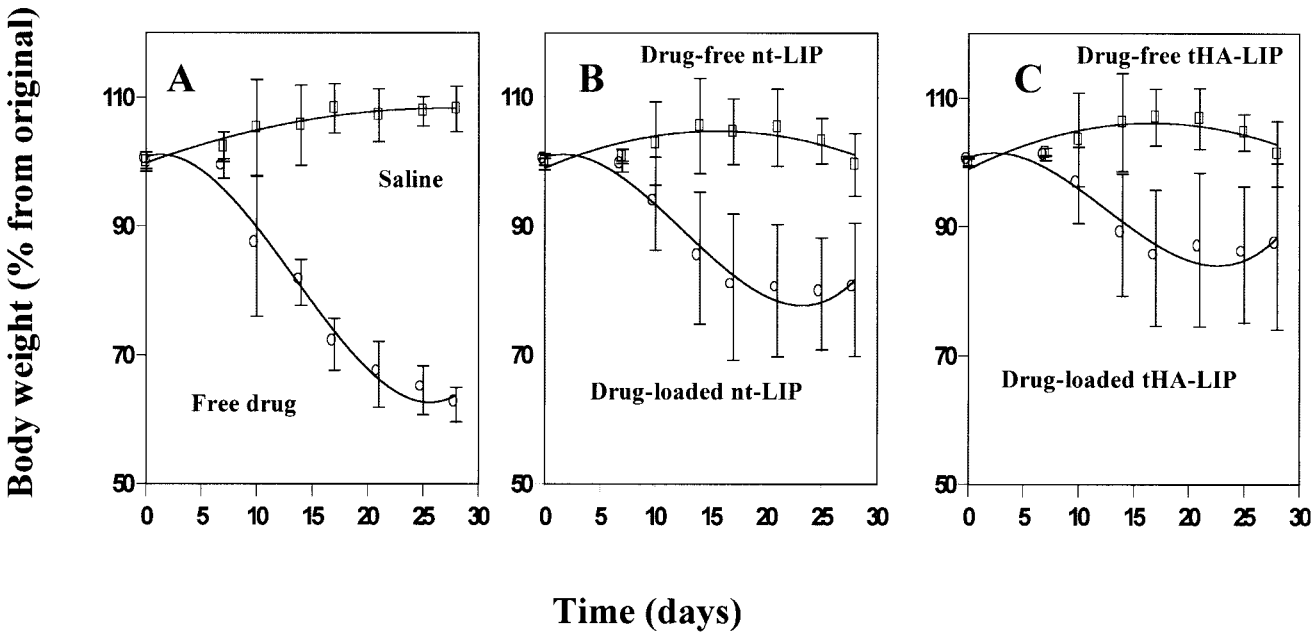

FIGURE 3 – The change in body weight of healthy mice over time ($n = 5$ per group) as function of injected material. (*a*) Free MMC vs. saline. (*b*) MMC encapsulated in nt-LIP *vs.* same, but drug-free, liposomes. (*c*) MMC encapsulated in tHA-LIP *vs.* same, but drug-free, liposomes. Each animal received 5 injections of the selected formulation into the tail vein, on Days 0, 7, 14, 21 and 28. The MMC dose in each injected formulation was 10 mg/Kg body. The points are the experimental data (each an average of 5 animals), the error bars represent the SD and the solid curves are non-theoretical, drawn to emphasize the trends in the data.

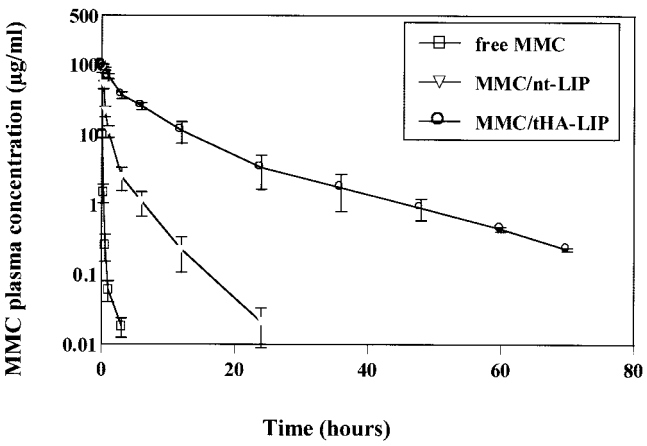

FIGURE 4 – MMC plasma concentration (μg/ml) as function of time from dosing, in C57BL/6 mice inoculated (by i.v. injection) with B16F10.9 cells ($n = 10$ per group). □, free MMC; ▽, MMC in nt-LIP; ○, MMC in tHA-LIP. A single dose of the selected formulation was injected to the tail vein and the MMC dose in each injected formulation was 10 mg/Kg body. The points are experimental, each an average from all animals in the group and the error bars represent the SD. The solid curves are non-theoretical, drawn to emphasize the trends in the data.

known to have receptors for HA[22,23] (Fig. 2). Free fluorescein was used as a liposome-encapsulated marker. Unencapsulated fluorescein was removed from the tested liposomal formulations and it was also verified that efflux of encapsulated fluorescein was negligible during the time span of these experiments (data not shown). Fluorescein-labeled HA, a marker sensitive to HA receptors, was positioned on the surface of the targeted liposomes and, for these experiments, the liposomes encapsulated buffer alone. Fluorescein was hardly detectable when incubated with cells either in free form (Fig. 2*a*,*i*) or encapsulated in nt-LIP (Fig. 2*a*,*ii*), whereas incubation with fluorescein-encapsulating tHA-LIP resulted in significant fluorescence at the cell membrane (Fig. 2*a*,*iii*), clearly indicative of binding. Further support that tHA-LIP bind to HA-receptors on the cell membranes can be seen in Figure 2*b*, from the side by side views of tHA-LIP carrying a liposomal surface marker (2*b*,*i*) and an internal aqueous marker (2*b*,*ii*).

Cellular cytotoxicity of MMC formulated in tHA-LIP

The studies were conducted with 6 cell lines, that fall into 2 categories with respect to expression of hyaluronan receptors. Four overexpress HA receptors: C-26 (mouse colon carcinoma[57]); B16F10.9 (mouse melanoma[22]); D122 (highly metastatic clone of Lewis lung carcinoma[59]); PANC-1 (human adenocarcinoma[15]). Two underexpress HA receptors: CV-1 (African green monkey kidney cells[60]); U2OS (human osteosarcoma). Normal cell growth and viability were unaffected by drug-free nt-LIP or tHA-LIP, and cellular response to free MMC was the same whether "empty" liposomes of either type were, or were not, suspended in the treatment media (data not shown). Irrespective of whether hyaluronan receptors were over- or underexpressed, treatment with free MMC had a slight advantage over treatment with MMC-loaded nt-LIP (Table I). Moreover, cells poor in hyaluronan receptors were insensitive to whether the liposomes were targeted or not (Table I). The situation changed markedly when cells that overexpress the hyaluronan receptor were treated with MMC- loaded tHA-LIP, the IC_{50} values dropped-down by 50–200-fold (Table I). These observations indicate the specificity of the tHA-LIP to hyaluronan receptors and demonstrate the advantages of tHA-LIP, over free drug and drug encapsulated in nt-LIP.

In vivo *subacute toxicity*

Mice injected with free drug lost weight, as expected (Fig. 3*a*). Animals injected with drug-free nt-LIP (Fig. 3*b*) or tHA-LIP (Fig. 3*c*) did not lose weight over the entire duration of the experiment and over the span of 5 injections, strongly indicating that both types of liposomes are not toxic to the animals. Encapsulation in liposomes modulated drug toxicity (Fig. 3*b*,*c*) compared to free

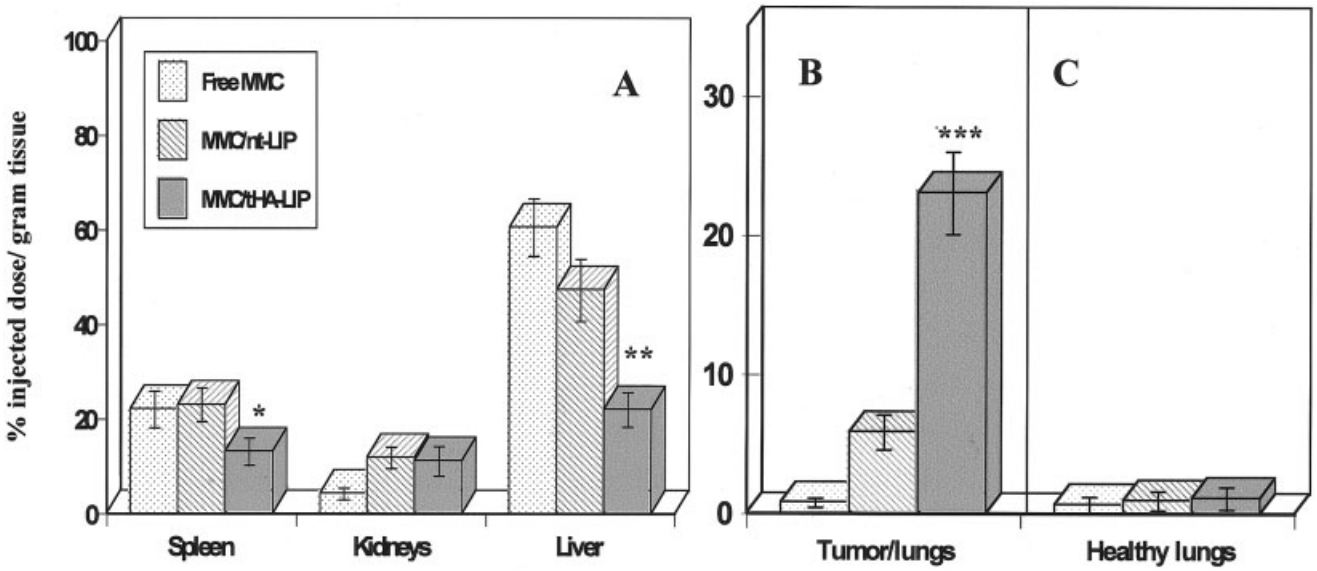

FIGURE 5 – Drug biodistribution (% of injected dose/gram tissue) in healthy and in B16F10.9 tumor-bearing C57BL/6 mice ($n = 5$ per group). Inoculation of tumor cells, MMC administration and dose were as listed under Figure 4. Dotted bars, free MMC; diagonal-stripe bars, MMC encapsulated in nt-LIP; dark-shaded bars, MMC encapsulated in tHA-LIP. Each bar is an average from all animals in the group and the error bars represent the SD. (*a*) Biodistribution in selected non-tumor bearing organs of B16F10.9 inoculated animals. (*b*) Biodistribution in the tumor-bearing lungs of B16F10.9 inoculated animals. (*c*) Biodistribution in the lungs of healthy animals. Statistical significance evaluations represented on the figure by stars are comparisons of selected formulation to free MMC. $*p < 0.05$; $**p < 0.01$; $***p < 0.001$.

MMC (Fig. 3*a*), tHA-LIP better than nt-LIP. Pathology examination of the selected organs fit with these findings.

Pharmacokinetics and biodistribution of free and of liposomal MMC in tumor-bearing C57BL/6 mice

Free MMC was rapidly eliminated from the circulation (Fig. 4). Formulating MMC in liposomes extended its retention in circulation, modestly by the nt-LIP and substantially by the tHA-LIP (Fig. 4). The AUC ratios tHA-LIP/nt-LIP and tHA-LIP/free MMC, were 9 and 91, respectively.

Pathology examination found tumors in the lungs of the animals injected with B16F10.9 cells, whereas their spleens, kidneys and livers were found to be tumor-free. The sequence of MMC uptake in the tumor-free organs was: free drug > nt-LIP > tHA-LIP (Fig. 5*a*). In liver and spleen, encapsulation in the tHA-LIP lowered MMC uptake significantly, compared to free drug ($p < 0.01$ and $p < 0.05$, respectively) and to MMC in the nt-LIP ($p = 0.047$ and $p = 0.045$, respectively). This sequence was reversed, tHA-LIP > nt-LIP > free drug, for MMC uptake into the tumor (Fig. 5*b*). Mediated by the tHA-LIP, drug uptake into tumor was 4-fold and 30-fold higher compared to nt-LIP ($p = 0.018$) and to free drug ($p < 0.001$), respectively. In contrast, drug uptake into the lungs of healthy animals was negligible (Fig. 5*c*) irrespective of whether the drug was free or formulated in liposomes (both types).

Therapeutic responses of mice bearing B16F10.9-originating lung metastatic disease. At 21 days, the average lungs weight of the normal healthy mice was 0.21($\pm$0.03) g. All mice inoculated with the tumor cells were found to have increased lung weights compared to the normal mice, but to different extent, depending on the treatment received. The metastatic burden was highest for the saline group by both measures of lung metastatic burden (Fig. 6*a*), the increase in lung weight over that of normal lungs (see above) and the number of lung metastasis. The burden remained high upon treatments with free drug or drug-encapsulating nt-LIP (Fig. 6*a*). Only treatment with the MMC-loaded tHA-LIP reduced the metastatic burden significantly ($p < 0.001$) (Fig. 6*b*): increase in lung weight was only 25% over normal lungs, with a concomitant small number (<10) of lung metastasis. These encouraging results were mirrored by the survival data (Fig. 6*b*). Treatment with MMC-loaded tHA-LIP generated a substantial and significant increase in survival ($p < 0.0007$ and $p < 0.001$) compared to free drug and to MMC-loaded nt-LIP, respectively.

Therapeutic responses of BALB/c mice bearing C-26 solid tumors

The pharmacokinetics were quite similar (data not shown) to those of the B16F10.9 model (Fig. 4). The AUC ratios tHA-LIP/nt-LIP and tHA-LIP/free MMC were 12 and 105, respectively.

Tumor volumes increased rapidly and exponentially when animals were treated with saline alone, free MMC or MMC-loaded nt-LIP (Fig. 7*a*), with little difference among these 3 treatment groups. Tumor was detectable in all these groups at Day 7 post-inoculation. Treatment with MMC-loaded tHA-LIP slowed tumor growth rate significantly. The tumors in these animals were smallest among all four groups, and were first detected on Day 13, close to 2-fold delay compared to all other groups. These results were also mirrored by the survival data (Fig. 7*b*). Treatment with MMC-loaded tHA-LIP was distinctly different that the other 3 groups, resulting in highly prolonged survival ($p < 0.0007$ and $p < 0.001$) compared to free drug and to drug-loaded nt-LIP, respectively.

Survival of C57BL/6 mice bearing D122-originating lung metastasis

The effects of the 4 treatment groups on the survival of animals bearing this highly aggressive Lewis Lung Carcinoma, which overexpresses hyaluronan receptors,[59] were similar to trends observed in the 2 other tumor models (Fig. 8). Survival rates of animals treated with saline, free MMC or MMC-loaded nt-LIP were quite poor, with slight differences from one treatment group to the other. Treatment with MMC-loaded tHA-LIP was quite effective in prolonging survival (Fig. 8) ($p < 0.0007$ and $p < 0.001$) compared to the other 2 drug formulations, respectively.

DISCUSSION

The therapeutic potential of MMC led us to use it as the drug of choice with which to pursue our working hypothesis that hyalu-

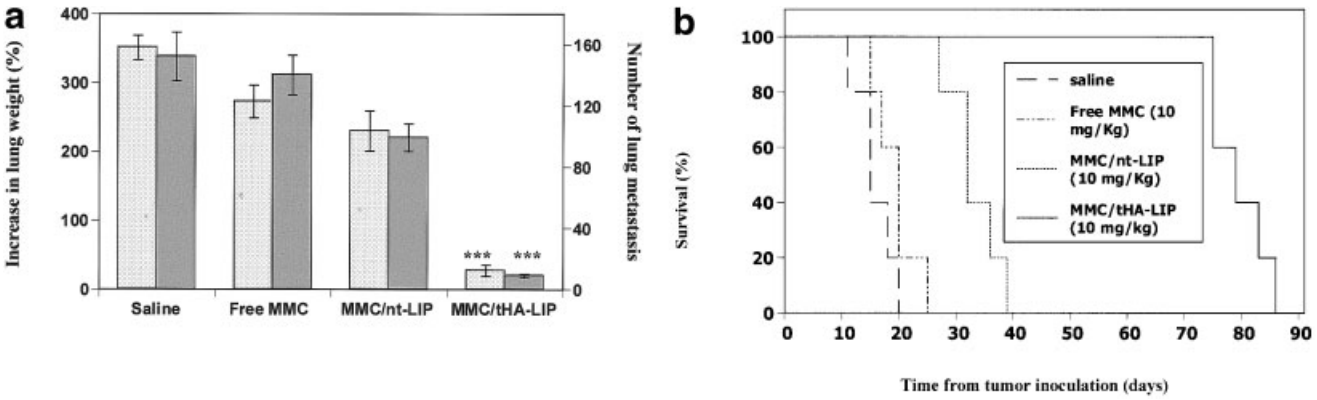

FIGURE 6 – Therapeutic responses of mice bearing B16F10.9-originating lung metastatic disease. The 4 treatment groups were: saline, free MMC, MMC encapsulated in nt-LIP and MMC encapsulated in tHA-LIP. Drug dose in all formulations was 10 mg/Kg body and treatments were on Days 1, 5, and 9, by injection of the selected formulation to the tail vein. (*a*) Lung metastatic burden. Light-shaded bars are the data for the increase in lung weight, dark-shaded bars are the data for the number of lung metastasis. Each bar is an average of all animals in the group ($n = 5$) and the SD are represented by the error bars. ***$p < 0.001$ compared to free drug. (*b*) Survival ($n = 7$). Each line connects the symbols representing the daily survival state of the group, the symbols themselves were omitted to avoid a cluttered figure.

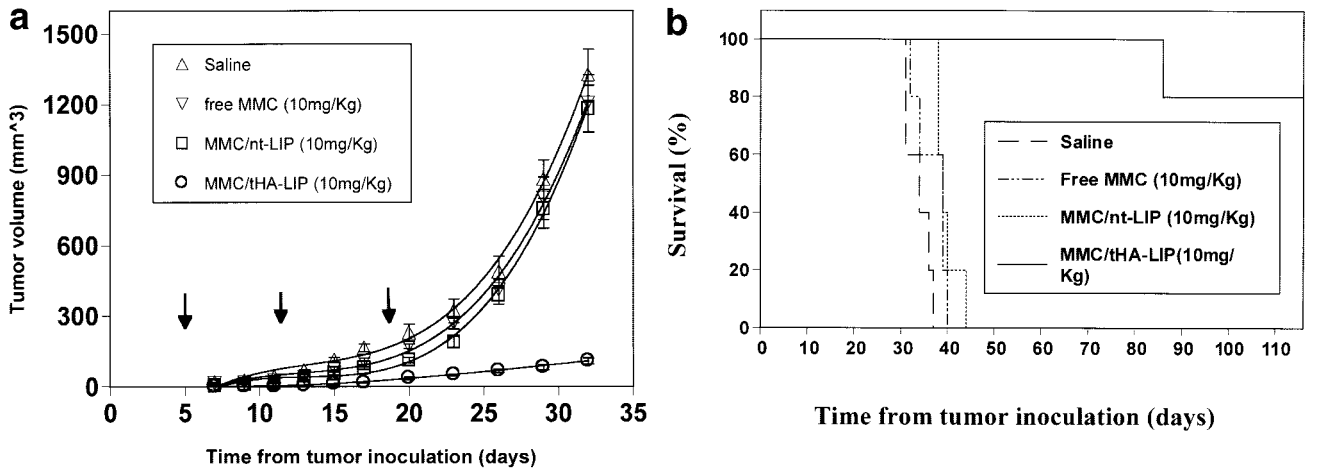

FIGURE 7 – Therapeutic responses of (BALB/c) mice inoculated with C-26 cells injected to the right-hind footpad. (*a*) Increase in tumor volume ($n = 20$ per group). Treatment groups, MMC formulations, doses, and administration route were as listed under Figure 6*a*. Treatments were on Days 5, 12 and 19 (indicated by the arrows). △, Saline; ▽, free MMC; □, MMC encapsulated in nt-LIP; ○, MMC encapsulated in tHA-LIP. The points are the experimental data, each an average of all animals in the group and the SEM are represented by the error bars. The solid curves are non-theoretical, drawn to emphasize the trends in the data. (*b*) Survival ($n = 10$ per group). Treatments were on Days 5, 12, 19 and 26. Lines representations are as defined under 6B.

ronan, positioned covalently at the surface of small liposomes allows for long-term circulation and for targeting to tumors. Using, as we have chosen, the naturally occurring high M_r ($\sim 10^6$ Da) hyaluronan, rather than hyaluronan fragments, provided 2 critical advantages. The complete macromolecule binds to hyaluronan receptors with higher affinity than hyaluronan fragments,[61] and provides long-term circulation through its many hydroxyl residues. A further advantage of hyaluronan-liposomes is our recent findings that hyaluronan also acts as a cryoprotectant.[52]

The low encapsulation levels (<5%) reported previously for liposomal MMC formulations,[48,49] dictated that our first task would center on efforts to improve this property. Using relatively high liposome concentrations at the stage of drug encapsulation, and our novel method of encapsulation,[51,52] resulted in a generous increase (up to 50%) of MMC encapsulation efficiency.

A major motivation to pursue carrier-mediated MMC formulations was the potential to reduce the toxicity of free MMC, but without introducing new, carrier-derived, risks of toxicity. The positive results for both drug-free and drug-loaded carrier formulations, using subacute MMC doses, obtained from the subacute toxicity studies in healthy mice (Fig. 3), made it feasible to proceed to the tumor-bearing mice.

MMC pharmacokinetics, as function of formulation species, was followed *in vivo* to evaluate one part of the working hypothesis, that the many hydroxyl residues present in hyaluronan would provide the liposomes with the hydrophilic coat needed for long-term retention in circulation. Encapsulation in the nt-LIP already enhanced retention in circulation compared to free drug (Fig. 4), probably due to the small size of these liposomes. Adding the hyaluronan coat was, however, the critical factor. It turned these small particles into long-circulating species, over a time frame similar to (or better than) was reported for PEG-coated liposomes.[25–30,53] Similar pharmacokinetics obtained in the C-26 bearing animals (data not shown) indicates that long-term circulation of hyaluronan-liposomes is not restricted to a single tumor model.

MMC biodistribution studies were carried out to test the second part of the working hypothesis, that the hyaluronan positioned covalently on the liposomal surface would endow these liposomes

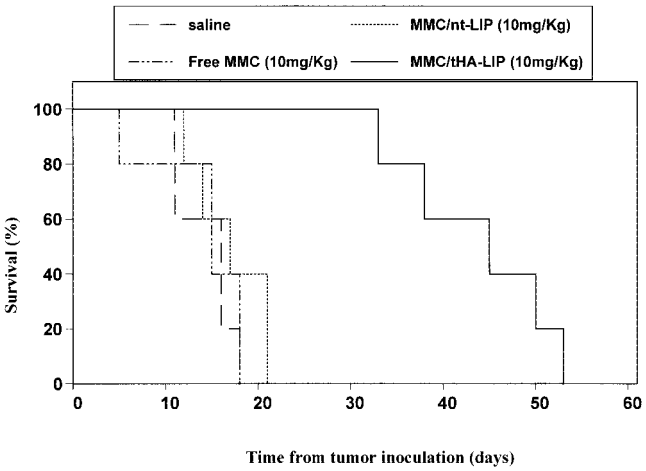

FIGURE 8 – Survival of C57BL/6 mice bearing D122-originating lung metastasis ($n = 5$). Treatment groups, MMC formulations, doses and administration route were as listed under Figure 6*a*. Lines representations are as defined under Figure 6*b*.

with the ability to truly mediate drug targeting to tumors. These expectations, affirming the working hypothesis, were clearly met. When delivered via tHA-LIP, MMC accumulation in the tumor was 30-fold higher than when the drug was administered in free form, and 4-fold higher than when delivered via nt-LIP (Fig. 5*a*,*b*). That the tumor, rather than the anatomic location, makes the difference, can be appreciated from the selectivity, defined as the ratio of drug uptake into the lungs of tumor-bearing mice, compared to the same organ in healthy (tumor-free) animals. We obtained a selectivity of 20 (Fig. 5*b*,*c*), which is higher than reported for doxorubicin encapsulating sterically stabilized regular and immunoliposomes.[62] Tumor-selectivity is also seen from the distribution to other organs in the tumor-bearing mice. MMC uptake into spleen and kidneys was not very sensitive to the nature of drug formulation, and liver uptake was significantly reduced when the drug was delivered via the tHA-LIP (Fig. 5*a*). These findings fits well with ability of these targeted liposomes to reduce the MMC-dependent subacute toxicity (Fig. 3).

The next rational step was to evaluate whether the long circulation and the targeting give rise to improved therapeutic responses. The *in vitro* studies already showed that loading into the tHA-LIP generates a 100-fold increase in MMC potency in tumor cells that overexpress hyaluronan receptors, but not in cells with poor expression of these receptors (Table I). These results made it obvious that *in vivo* studies should focus only on tumor models based on cells overexpressing hyaluronan receptors.

Similar to the *in vitro* results but, much more relevant trends, were found when the systems were subjected to *in vivo* testing. Taking together the measures of tumor response to treatment (Figs. 6–8), tumor size, metastatic burden and survival, treatments with free MMC were not much different than no treatment. The responses to treatment with MMC-loaded nt-LIP were only a slight improvement over free drug or no treatment. On this low background, we find the highly positive responses to treatment with MMC-loaded tHA-LIP, quite striking.

Although the time span of long circulation we achieved is in the range reported for other long-circulating liposomes, our tHA-LIP slowed-down tumor progression with concomitant smaller tumors, and increased life span (compared to treatment with free drug), better than sterically-stabilized liposomes in similar and in other mouse tumor models but with other anticancer drugs.[53,63–65]

We suggest that the encouraging results reported here stem from combination of all attributes of this formulation: good encapsulation, sustained release, long retention in circulation and high-affinity binding to the tumor, allowing the liposomes to act there as sustained-release drug depots. Another factor that may have contributed to the positive outcome, could come from the hyaluronan itself. It has been suggested that hyaluronan receptors in tumor cells are involved in tumor progression, allowing tumor cells to interact with hyaluronan in the extracellular matrix.[5,7,8,10–12,14–17] For example, administration of hyaluronan fragments to block the hyaluronan receptors of tumor cells was shown to slow down tumor progression.[22] It can be speculated that when the tHA-LIP bind to the hyaluronan receptors at the tumor, they perform 2 roles: act as a depot of the chemotherapeutic drug and at the same time slow down tumor progression by blocking the receptors.

In conclusion, formulation of MMC in the tHA-LIP may make it possible to salvage the therapeutic potential of this drug, thereby increasing the arsenal of anticancer drugs available for the patient. The tHA-LIP emerge as a valid option for tumor chemotherapy, worthy of further pursuit, with a distinct advantages: cryoprotection,[52] long circulation and high affinity to the target, provided by the same single (naturally-occurring) agent, anchored to the liposomal surface.

ACKNOWLEDGEMENTS

The authors wish to thank Dr. A. Barbul from TAU Confocal Microscopy Unit. Dr. D. Stephansky from the Hebrew University, Jerusalem. Dr. A. Nechmad, Dr. N. Cohen, Mr. Y. Dekel, Ms. D. Melikhov and Ms. A. Florentin, from Tel Aviv University for their help in the animal experiments. Dr. N. Yerushalmi from Tel Aviv University for helpful discussion and comments.

REFERENCES

1. O'Regan M, Martini I, Crescenzi F, De Luca C, Lansing M. Molecular mechanisms and genetics of hyaluronan biosynthesis. Int J Biol Macromol 1994;16:283–6.
2. Baker JR, Caterson B. Radioimmunoassay of the link proteins associated with bovine nasal cartilage proteoglycan. J Biol Chem1 1979; 254:9369–72.
3. LeBaron RG, Zimmermann DR, Ruoslahti E. Hyaluronate binding properties of versican J Biol Chem 1992;267:10003–10.
4. Rauch U, Karthikeyan, L, Maurel P, Margolis RU, Margolis RK. Cloning and primary structure of neurocan, a developmentally regulated, aggregating chondroitin sulfate proteoglycan of brain. J Biol Chem 1992;267:19536–47.
5. Zöller M. CD44: physiological expression of distinct isoforms as evidence for organ-specific metastasis formation. J Mol Med 1995; 73:425–38.
6. Smadja-Joffe F, Legras S, Girard N, Li Y, Delpech B, Bloget F, Morimoto K, Le Bousse-Kerdiles C, Clay D, Jasmin C, Levesque JP. CD44 and hyaluronan binding by human myeloid cells. Leuk Lymphoma 1996;21:407–20.
7. Rudzki Z., Jothy S. CD44 and the adhesion of neoplastic cells. Mol Pathol 1997;50:57–71.
8. Sneath RJ, Mangham DC. The normal structure and function of CD44 and its role in neoplasia. Mol Pathol 1998;51:191–200.
9. Borland G, Ross JA, Guy K. Forms and functions of CD44. Immunology 1998;93:139–48.
10. Herrera-Gayol A, Jothy S. Adhesion proteins in the biology of breast cancer: contribution of CD44. Exp Mol Pathol 1999;66:149–56.
11. Tran TA, Kallakury BV, Sheehan CE, Ross JS. Expression of CD44 standard form and variant isoforms in non-small cell lung carcinomas. Hum Pathol 1997;28:809–14.
12. Fasano M, Sabatini MT, Wieczorek R, Sidhu G, Goswami S., Jagirdar J. CD44 and its v6 spliced variant in lung tumors: a role in histogenesis? Cancer 1997;80:34–41.
13. Gallatin M , St. John TP, Siegelman M, Reichert R, Butcher EC, Weissman IL. Lymphocyte homing receptors. Cell 1986;44:673–80.
14. Li H, Guo L, Li JW, Liu N, Qi R, Liu J. Expression of Hyaluronan receptors CD44 and RHAMM in stomach cancers: relevance with tumor progression. Int J Oncol 2000;17:927–32.
15. Abetamann V, Kern HF, Elsasser HP. Differential expression of the hyaluronan receptors CD44 and RHAMM in human pancreatic cancer cells. Clin Cancer Res 1996;2:1607–18.
16. Ahrens T, Assmann V, Fieber C, Termeer C, Herrlich P, Hofmann M,

Simon JC. CD44 is the principal mediator of hyaluronic-acid-induced melanoma cell proliferation. J Invest Dermatol 2001;116:93–101.
17. Ohene-Abuakwa Y, Pignatelli M. Adhesion molecules in cancer biology. Adv Exp Med Biol 2000;465:115–26.
18. Penno MB, August JT, Baylin SB, Mabry M, Linnoila RI, Lee VS, Croteau D, Yang XL, Rosada C. Expression of CD44 in human lung tumors. Cancer Res 1994;54:1381–7.
19. Birch M, Mitchell S, Hart IR. Isolation and characterization of human melanoma cell variants expressing high and low levels of CD44. Cancer Res 1991;51:6660–7.
20. Bartolazzi A, Peach R, Aruffo A, Stamenkovic I. Interaction between CD44 and hyaluronate is directly implicated in the regulation of tumor development. J Exp Med 1994;180:53–66.
21. Lesley J, Hyman R. CD-44 structure and function. Frontiers in Bioscience, 1998;3:D616–30.
22. Zeng C, Toole BP, Kinney SD, Kuo JW, Stamenkovic I. Inhibition of tumor growth *in vivo* by hyaluronan oligomers. Int J Cancer 1998;77: 396–401.
23. Zawadzki V, Perschl A, Rösel M, Hekele A, Zöller M. Blockade of metastasis formation by CD44-receptor globulin. Int J Cancer 1998; 75:919–24.
24. Sy MS, Guo YJ, Stamenkovic I. Inhibition of tumor growth *in vivo* with a soluble CD44-immunoglobulin fusion protein. J Exp Med 1992;176:623–7.
25. Gabizon AA. Pegylated liposomal doxorubicin:metamorphosis of an old drug into a new form of chemotherapy. Cancer Invest 2001;19:424–36.
26. Moghimi SM, Hunter AC, Murray JC. Long-circulating and target-specific nanoparticles: theory to practice. Pharmacol Rev 2001;53: 283–318.
27. Forssen AE, Coulter DM, Proffit RC. Selective localization of daunorubicin small unilamellar vesicles in solid tumors. Cancer Res 1992; 52:3255–61.
28. Allen TM. Long-circulating (sterically stabilized) liposomes for targeted drug delivery Trends Pharmacol Sci 1994;15:215–20.
29. Oku N, Namba Y. Long-circulating liposomes. Crit Rev Ther Drug Carrier Syst 1994;11:231–70.
30. Tardi P. Choice E, Masin D, Redelmeier T, Bally M, Madden TD. Liposomal encapsulation of topotecan enhances anticancer efficacy in murine and human xenograft models. Cancer Res 2000;60:3389–93.
31. Tseng YL, Hong RL, Tao MH, Chang FH. Sterically stabilized anti-idiotype immunoliposomes improve the therapeutic efficacy of doxorubicin in a murine B-cell lymphoma mode. Int J Cancer 1999; 80:723–30.
32. Koning GA, Morselt HW, Gorter A, Allen TM, Zalipsky S, Kamps JA, Scherphof GL. Pharmacokinetics of differently designed immunoliposome formulations in rats with or without hepatic colon cancer metastases. Pharm Res 2001;18:1291–8.
33. Yerushalmi N, Margalit R. Bioadhesive, collagen-modified liposomes: molecular and cellular level studies on the kinetics of drug release and on binding to cell monolayers. Biochim Biophys Acta 1994;1189:13–20.
34. Yerushalmi N, Margalit R. Hyaluronic acid-modified bioadhesive liposomes as local drug depots: effects of cellular and fluid dynamics on liposome retention at target sites. Arch Biochem Biophys 1998; 349:21–6.
35. Yerushalmi N, Arad A, Margalit R. Molecular and cellular studies of hyaluronic acid-modified liposomes as bioadhesive carriers for topical drug delivery in wound healing. Arch Biochem Biophys 1994;313:267–73.
36. Margalit R. Liposome-mediated drug targeting in topical and regional therapies. Crit Rev Ther Drug Carrier Syst 1995;12:233–61.
37. Margalit R, Okon M, Yerushalmi N, Avidor E. Bioadhesive liposomes for topical drug delivery: molecular and cellular studies. J Cont Rel 1992;19:275–88.
38. Margalit, R. Bioadhesive liposomes in topical treatment of wounds. In: Cohen S, Berenstein H, eds. Microparticulates: preparation, characterization and application in medicine. New York: Marcel Dekker Inc., 1996. 425–61.
39. Carter SK, Crooke ST. Mitomycin C: current status and new developments. New York: Academic Press, 1979.
40. Hinoshita E, Uchiumi T, Taguchi K, Kinukawa N, Tsuneyoshi M, Sugimachi K, Kuwano M. Increased expression of an ATP-binding cassette superfamily transporter, multidrug resistance Protein 2, in human colorectal carcinomas. Clin Cancer Res 2000;6:2401–7.
41. Dalton JT, Wientjes MG, Badalament RA, Drago JR, Au JL. Pharmacokinetics of intravesical mitomycin C in superficial bladder cancer patients. Cancer Res 1991;51:5144–52.
42. Chang MR, Cheng QI, Lee DA. Basic science and clinical aspects of wound healing in Glaucoma filtering surgery. J Ocul Pharmacol Ther 1998;14:75–95.
43. Tahery MM, Lee DA. Pharmacologic control of wound healing in Glaucoma filtration surgery. J Ocul Pharmacol 1989;5:155–179.
44. Yoshimoto M, Saito M, Tada T, Kasumi KT. Unexpected increase in the bone marrow toxicity of mitomycin C (MMC). Br J Cancer 2001;84:736–7.
45. Tokunaga Y, Kagayama A. Liposomal sustained release delivery systems for intravenous injection. I, Physicochemical and biological properties of newly synthesized lipophilic derivatives of Mitomycin C. Chem Pharmacol Bull 1988;36:3060–9.
46. Sasaki H, Hashida M, Sezaki H. Characterization of liposomes and emulation containing Mitomycin C or lipophilic prodrugs. J Pharm Sci 1986;75:1166–70.
47. Sasaki H, Hashida M, Sezaki H. Absorption characteristics of lipophilic prodrug of Mitomycin C from injected liposomes or an emulsion. J Pharm Sci 1985;37:461–5.
48. Tsai DC, Howard SA, Hogan TF, Malanga CJ, Kandzari SJ, Ma JKH. Preparation and *in vitro* evaluation of polylactic acid-mitomycin C microcapsules. J Microencapsul 1986;3:181–93.
49. Whateley TL, Eley JG, Kerr DJ, McArdle CS, Anderson J, Vert M, Davis SS. Incorporation of mitomycin C into microspheres of biodegradable poly (lactide-glycolide) co-polymers. Abstr Pap Am Chem Soc 1992;203:59.
50. Cummings J, Allan L, Smyth JF. Encapsulation of mitomycin C in albumin microspheres markedly alters pharmacokinetics. Biochem Pharmacol 1994;47:1345–56.
51. Peer D, Margalit R. Physicochemical evaluation of a stability-driven approach to drug entrapment in regular and in surface-modified liposomes. Arch Biochem Biophys 2000;383:185–90.
52. Peer D, Florentin A, Margalit R. Hyaluronan is a key component of cryoprotection and formulation of targeted unilamellar liposomes. Biochim Biophys Acta 2003;1612:76–82.
53. Hong RL, Huang CJ, Tseng YL, Pang V, Chen ST, Liu JJ, Chang FH. Direct comparison of liposomal doxorubicin with or without polyethylene glycol coating in C-26 tumor-bearing mice: is surface coating with polyethylene glycol beneficial? Clin Cancer Res 1999;5:3645–52.
54. Lin P, Buxton JA, Acheson A, Radziejewski C, Maisonpierre PC, Yancopoulos GD, Channon KM, Hale LP, Dewhirst MW, George SE, Peters KG. Antiangiogenic gene therapy targeting the endothelium-specific receptor tyrosine kinase Tie2. Proc Natl Acad Sci USA 1998;21:8829–34.
55. Goldman Y, Peled A, Shinitzky M. Effective elimination of lung metastases induced by tumor cells treated with hydrostatic pressure and *N*-acetyl-L-cysteine. Cancer Res 2000;60:350–8.
56. Mosmann T. Rapid colorimetric assay for cellular growth and survival: application to proliferation and cytotoxicity assays. J Immun Methods 1983;65:55–63.
57. Samuelsson C, Gustafson S. Studies on the interaction between hyaluronan and a mouse colon cancer cell line. Glycoconj J 1998;15: 169–75.
58. Lokeshwar VB, Iida N, Bourguignon LYW. The cell adhesion molecule, GP116, is a new CD44 variant (ex14/v10) involved in hyaluronic acid binding and endothelial cell proliferation. J Biol Chem 1996;271:23853–64.
59. Hofmann M, Fieber C, Assmann V, Gottlicher M, Sleeman J, Plug R, Howells N, von Stein O, Ponta H, Herrlich P. Identification of IHABP, a 95 kDa intracellular hyaluronate binding protein. J Cell Sci 1998;111:1673–84.
60. Eliaz RE, Szoka FC Jr. Liposome-encapsulated doxorubicin targeted to CD44: a strategy to kill CD44-overexpressing tumor cells. Cancer Res 2001;61:2592–601.
61. Karvinen S, Kosma VM, Tammi MI, Tammi R. Hyaluronan, CD44 and versican in epidermal keratinocyte tumours. Br J Dermatol 2003; 148:86–94.
62. Emanuel N, Kedar E, Bolotin EM, Smorodinsky NI, Barenholz Y. Targeted delivery of doxorubicin via sterically stabilized immunoliposomes: pharmacokinetics and biodistribution in tumor-bearing mice. Pharm Res 1996;13:861–8.
63. Newman MS, Colbern GT, Working PK, Engbers C, Amantea MA. Comparative pharmacokinetics, tissue distribution, and therapeutic effectiveness of cisplatin encapsulated in long-circulating, pegylated liposomes (SPI-077) in tumor-bearing mice. Cancer Chemother Pharmacol 1999;43:1–7.
64. Charrois JRG, Allen TM. Rate of biodistribution of STEALTH® liposomes to tumor and skin: influence of liposome diameter and implications for toxicity and therapeutic activity. Biochim Biophys Acta 2003;1609:102–8.
65. Junping W, Maitani Y, Takayama K, Nagai T. In vivo evaluation of doxorubicin carried with long circulating and remote loading proliposome. Int J Pharm 2000;203:61–9.